Citation: Bucha B., Janák J. (2014) A MATLAB-based graphical user interface program for computing functionals of the geopotential up to ultra-high degrees and orders: Efficient computation at irregular surfaces, *Computers & Geosciences* 66, 219–227, DOI: 10.1016/j.cageo.2014.02.005

A MATLAB-based graphical user interface program for computing functionals of the geopotential up to ultra-high degrees and orders: efficient computation at irregular surfaces[☆]

Blažej Bucha[a,*], Juraj Janák[a]

[a]*Department of Theoretical Geodesy, Faculty of Civil Engineering, Slovak University of Technology in Bratislava, Radlinského 11, 813 68 Bratislava 15, Slovakia*

Abstract

Fast spherical harmonic synthesis (SHS) at multiple points based on the lumped coefficients approach is very well-established technique. However, this method cannot be applied to SHS at irregular surfaces, as the points must be regularly spaced and refer to a regular surface such as the sphere or the ellipsoid of revolution. In this paper we present a MATLAB®-based graphical user interface software for ultra-high degree SHS on grids at irregular surfaces, like the Earth surface. This software employs the highly efficient lumped coefficient approach for SHS at regular surfaces and the Taylor series expansions to continue the functionals to the irregular surfaces, e.g. the Earth surface. The generalized idea of continuing functionals using the Taylor series was presented by Hirt (Journal of Geodesy 86:729–744, 2012). We took the advantage of the software GrafLab

[☆]Code available from `http://www.svf.stuba.sk/en/departments/department-of-theoretical-geodesy/science-and-research/downloads.html?page_id=4996`

[*]Corresponding author. Tel.: +421 2 59274342; fax: +421 2 52925476.

Email addresses: `blazej.bucha@stuba.sk` (Blažej Bucha), `juraj.janak@stuba.sk` (Juraj Janák)

(Bucha and Janák in Computers & Geosciences 56:186–196, 2013), which employs the lumped coefficients approach, and developed a new software isGrafLab (Irregular Surface GRAvity Field LABoratory). Compared to the commonly used "two loops" approach, the factor of increased computational speed can reach a value of several hundreds. isGrafLab allows accurate evaluation of 38 functionals of the geopotential on grids at irregular surfaces. High orders of the Taylor series can be used for the continuation. The new software offers all the other options available in GrafLab, such as the employment of three different approaches to compute the fully normalized associated Legendre functions, the graphical user interface or the possibility to depict data on a map.
Keywords: Geopotential model, Gravity field functional, Spherical harmonic synthesis, Lumped coefficients, Irregular surface, Taylor series

1. Introduction

In geosciences, the spherical harmonics (e.g. Freeden and Schreiner, 2009; Hobson, 1931; Hoffmann-Wellenhof and Moritz, 2005), which form orthonormal basis functions with a global support on the sphere, are frequently used to represent scalar fields such as the Earth gravitational (e.g. Pavlis et al., 2012) or magnetic (e.g. Finlay et al., 2010) field. By means of the spherical harmonics, these fields can be transformed from spatial domain into frequency domain (spherical harmonic analysis (SHA), e.g. Colombo (1981); Sneeuw (1994)), in which they are characterized by a set of spherical harmonic coefficients. These coefficients can be transformed back into the spatial domain (spherical harmonic synthesis (SHS), e.g. Barthelmes (2013); Fantino and Casotto (2009)), and in the case of the gravitational field one gets the gravitational potential (in short geopotential).

After applying some operator to the spherical harmonics (e.g. the pseudodifferential operators (cf. Freeden and Schreiner, 2009)), commonly used functionals of the geopotential can easily be obtained (e.g. gravitational tensor). When introducing the normal gravity field (cf. Hoffmann-Wellenhof and Moritz, 2005), functionals of the distrubing potential are easy to calculate as well (e.g. gravity anomaly, deflections of the vertical, geoid undulation, etc.).

Nowadays, the gravity field of the Earth is very well-known up to a certain level of frequencies, i.e. up to some degrees of spherical harmonics to which a certain spatial resolution corresponds. Global geopotential models of the Earth (GGMs) consist of spherical harmonic coefficients representing the Earth's gravitational field and of a few additional constants. Nowadays, GGMs are almost routinely used in geodesy and other geosciences (climatology, geology, geomorphology, geophysics, oceanography, etc.). As high-resolution GGMs we would like to mention EGM2008 (Pavlis et al., 2012) up to degree 2190, EIGEN-6C (Förste et al., 2011) up to 1420 and EIGEN-6C2 (Förste et al., 2012) up to 1949.

Certainly the most difficult part of the SHS is the numerical evaluation of high degree and order spherical harmonics, viz. the fully normalized associated Legendre functions of the first kind (fnALFs) (see e.g. Hoffmann-Wellenhof and Moritz, 2005). Since fnALFs cover a huge range of magnitude, underflow and overflow problems occur in their evaluation (Holmes and Featherstone, 2002). A lot of attention has been put on accurate and fast computation of these functions in the last decades. These efforts resulted in the development of several approaches to compute fnALFs, differing mainly in numerical stability and efficiency (Balmino et al., 2012; Fukushima, 2012a,b; Gruber et al., 2011; Holmes and Featherstone, 2002; Cheong et al., 2012; Jekeli et al., 2007; Nesvadba, 2009; Smith et al., 1981;

Šprlák, 2011; Wenzel, 1998).

In order to resolve the other problem of SHS, i.e. the numerical efficiency of computation, one frequently uses the well-known lumped coefficients approach (LCA), see Section 2.1 and the references therein. This method allows performing very fast SHS on the grids that are regularly spaced and refer to a regular surface (the sphere or the ellipsoid of revolution). However, this approach cannot be applied if one of these conditions is not fulfilled. Hirt (2012) recently presented an effective method, in which one of these conditions, namely the regularity of the surface, can be omitted. He generalized the approach published already by Rapp (1997), who utilized the first-order Taylor series to continue the height anomaly from the ellipsoid to the Earth surface. In other words, certain functional and its derivatives of chosen order can be computed on the sphere or the ellipsoid employing the LCA, and subsequently continued to an irregular surface, e.g. the Earth surface. This approach is very simple in principle, but it can also be highly efficient and accurate, as it will be pointed out. Basically an identical approach was employed in Balmino et al. (2012), Section 4.3 and Appendix B.

Various computer programs for computing functionals of the geopotential are available, e.g. Adams and Swarztrauber (1997); Barthelmes (2003); Holmes and Pavlis (2008); Janák and Šprlák (2006); Sanso and Sona (2001); Smith (1998); Tscherning et al. (1983); Wieczorek (2012); Wittwer et al. (2008) or recently published Bucha and Janák (2013). A software to compute elements of the disturbing tensor on grids at irregular surfaces was presented by Eshagh and Abdollahzadeh (2012). However, to the knowledge of the authors, there is no compact and publicly available software with implemented accelerated routines that would allow fast and accurate SHS on grids at irregular surfaces such as the Earth surface.

This obstacle one usually circumvents by the point-wise approach with two loops, which can be, however, slower by a factor of several hundreds. This led us to modify the software GrafLab 1.1.2 (Bucha and Janák, 2013) to provide fast and accurate ultra-high degree SHS of functionals at irregular surfaces. The new software is called isGrafLab (Irregular Surface GRAvity Field LABoratory). It is written in MATLAB® and equipped with an easy-to-use graphical user interface, therefore no modifications on the source code level are necessary, as it is in the vast majority of the software of this kind.

The paper is organized as follows. Section 2 provides a brief recapitulation of the lumped coefficient approach and description of the Taylor expansions in the context of SHS at irregular surfaces. Section 3 describes the basic principles of manipulation with the software, and assessment of the accuracy and efficiency of the developed program. Summary and conclusions are presented in Section 4.

2. Spherical harmonic synthesis at irregular surfaces

2.1. Lumped coefficients approach

Disturbing potential (see e.g. Hoffmann-Wellenhof and Moritz, 2005) expanded into the truncated series of the spherical harmonics and written in the form that employs the lumped coefficients (e.g. Colombo, 1981; Fantino and Casotto, 2009) reads

$$T(r,\theta,\lambda) = \frac{GM}{r}\sum_{m=0}^{M}\left(A_m(\theta)\,\cos m\lambda + B_m(\theta)\,\sin m\lambda\right)\,, \tag{1}$$

where

$$A_m(\theta) = \sum_{n=m}^{M}\left(\frac{R}{r}\right)^n \bar{C}_{nm}\,\bar{P}_{nm}(\cos\theta)\,, \tag{2a}$$

$$B_m(\theta) = \sum_{n=m}^{M}\left(\frac{R}{r}\right)^n \bar{S}_{nm}\,\bar{P}_{nm}(\cos\theta)\,, \tag{2b}$$

and r, θ, λ denotes the spherical radius, the spherical co-latitude and the longitude, respectively, GM is the geocentric gravitational constant, R is the radius of the reference sphere, $\{\bar{C}_{nm}, \bar{S}_{nm}\}$ is the set of fully normalized spherical harmonic coefficients of degree n and order m (we assume that the spherical harmonic coefficients of the normal field have been substracted, see e.g. Barthelmes (2013), Eqs. (109) and (111)), $\bar{P}_{nm}(\cos\theta)$ are the fully normalized associated Legendre functions of the first kind (fnALFs) of degree n and order m, M denotes the maximum degree of spherical harmonic expansion and, finally, $A_m(\theta)$ and $B_m(\theta)$ stand for the lumped coefficients of the order m.

The efficiency of the LCA is in the fact that these coefficients (see Eqs. (2a) and (2b)) are constant along parallels in the grid, i.e. independent of the longitude. Therefore if one uses the standard co-latitude–longitude grid at the sphere or the ellipsoid of revolution, they need to be computed only once. Another trick is that both summations, i.e. over m and subsequently over n, can be summed by matrix multiplications, which significantly reduces the computation time. For the full vector-matrix notation of Eq. (1) see e.g. Bucha and Janák (2013).

An arbitrary functional of the geopotential can be written in the form of the lumped coefficients, and thus significantly speeds up (in some cases by a factor of several hundreds) SHS at regular surfaces.

2.2. Gradient approach in spherical coordinates

From Section 2.1 it is clear that the LCA cannot be applied to SHS on grids at the Earth surface, as the topography is varying differently in each meridian, and thus the coefficients $A_m(\theta)$ and $B_m(\theta)$ are not constant. An accurate, effective and very simple approach how to circumvent this issue has been proposed and verified by Hirt (2012), see also Balmino et al. (2012). They used Taylor expansions

(gradient approach) to continue functionals from regular surface, at which the LCA is employed, to irregular surface.

Let $P(r, \theta, \lambda) \in \Sigma$ be points of the standard co-latitude–longitude grid lying at the Earth surface Σ (or at an arbitrary irregular surface in general), and $P_0(r_0, \theta, \lambda) \in S$ be points of the same grid referring to the sphere S with the radius r_0. To continue disturbing potential from the points $P_0(r_0, \theta, \lambda) \in S$ to $P(r, \theta, \lambda) \in \Sigma$, the truncated Taylor series can be written in the form

$$T(r, \theta, \lambda) = T_0(r_0, \theta, \lambda) + \sum_{k=1}^{K} \frac{1}{k!} \frac{\partial^k T}{\partial r^k}\bigg|_{P_0(r_0,\theta,\lambda)\in S} (r - r_0)^k \,, \tag{3}$$

where K is the maximum order of the Taylor series. The k^{th} radial derivative of the disturbing potential can be obtained by the simple formula

$$\frac{\partial^k T(r, \theta, \lambda)}{\partial r^k} = (-1)^k \frac{GM}{r^{k+1}} \sum_{m=0}^{M} \left(A_m^{(k)} \cos m\lambda + B_m^{(k)} \sin k\lambda \right) , \tag{4}$$

in which

$$A_m^{(k)} = \sum_{n=m}^{M} \left(\frac{R}{r}\right)^n \left(\prod_{i=1}^{k} (n + i) \right) \bar{C}_{nm} \bar{P}_{nm}(\cos\theta) \,, \tag{5a}$$

$$B_m^{(k)} = \sum_{n=m}^{M} \left(\frac{R}{r}\right)^n \left(\prod_{i=1}^{k} (n + i) \right) \bar{S}_{nm} \bar{P}_{nm}(\cos\theta) \,. \tag{5b}$$

These equations employ the highly efficient LCA. After easy calculations, commonly used functionals of the geopotential can be continued to irregular surfaces using this scheme. Similar formulae for the gravity disturbance, the height anomaly and the deflections of the vertical can be found in Hirt (2012).

It is obvious that increasing the maximum order of the Taylor series will lead to better approximation of the functional. Until now, no approximation has been done, except for the truncation of the Taylor series at some finite order value K. However, as it will be pointed out in Section 3.2, in the "gradient approach in

spherical coordinates" sufficiently high order K ensures negligible approximation errors.

2.3. Gradient approach in ellipsoidal coordinates

An approximation is necessary, if one uses the ellipsoidal coordinates (φ, λ, h), i.e. the ellipsoidal latitude, the longitude and the ellipsoidal height, respectively, as input data instead of the spherical coordinates (r, θ, λ). The ellipsoidal coordinates of points $P(\varphi, \lambda, h) \in \Sigma$ at the standard latitude–longitude grid can be easily transformed into the spherical coordinates $P(r^E, \theta^E, \lambda) \in \Sigma$ by the well-known formulae (e.g. Hoffmann-Wellenhof and Moritz, 2005). However, due to the various values of h used in the original grid, the transformed co-latitudes θ^E vary along ellipsoidal parallels. Thus, the LCA cannot be applied. To ensure that θ^E will be constant along the parallels, some ellipsoid E at the ellipsoidal height h_0 above the reference ellipsoid can be used (h_0 can be e.g. average value computed from the minimum and the maximum ellipsoidal heights of the grid points), so that after the transformation one gets $P_0(r_0^E, \theta_0^E, \lambda) \in E$. The spherical co-latitudes θ_0^E are now constant along each parallel and the LCA can be employed. Functionals are therefore continued from the ellipsoidal surface $E \ni P_0(r_0^E, \theta_0^E, \lambda)$ to the Earth surface $\Sigma \ni P(r^E, \theta^E, \lambda)$.

The truncated Taylor expansion of disturbing potential reads

$$T(r^E, \theta^E, \lambda) \approx T_0(r_0^E, \theta_0^E, \lambda) + \sum_{k=1}^{K} \frac{1}{k!} \frac{\partial^k T}{\partial r^k}\bigg|_{P_0(r_0^E, \theta_0^E, \lambda) \in E} (h - h_0)^k \,. \tag{6}$$

The approximate sign in Eq. (6) is used because of the gradients computed in the radial direction, which differ from the gradients in the direction of $h - h_0$. This is, however, acceptable, as it was shown in Hirt (2012) and will be shown in Section 3.2 as well. Unlike the "gradient approach in spherical coordinates",

this also causes that beyond certain value of K, incessantly increasing the order of the Taylor series will not have the effect of permanently "better" and "better" approximation of the true value. In other words, the Taylor series converges, but to a value of the functional at slightly different point, and not to the true value.

2.4. Remark on the gradient approach of some functionals

Let us mention a short remark on the gradient approach of some functionals, e.g. the height anomaly, the components of deflection of the vertical, etc. These quantities are composite functions, because of the normal gravity γ (e.g. Hoffmann-Wellenhof and Moritz, 2005), which is also dependent on r. Thus, the truncated Taylor series for, let's say, the height anomaly reads ("approach in the spherical coordinates")

$$\zeta(r,\theta,\lambda) = \zeta_0(r_0,\theta,\lambda) + \sum_{k=1}^{K} \frac{1}{k!} \left. \frac{\partial^k T/\gamma}{\partial r^k} \right|_{P_0(r_0,\theta,\lambda)\in S} (r-r_0)^k \,. \tag{7}$$

When $k > 2$, the partial derivatives of the term T/γ significantly complicate numerical computation of Eq. (7), as both the disturbing potential T and the normal gravity γ are dependent on r. A very simple way how to avoid this problem, which was used in isGrafLab, is that the functional and its derivatives can be computed on the grid without the term $\gamma(r_0,\theta)$, and subsequently continued to the Earth surface. After this, the intermediate result is divided by $\gamma(r,\theta)$ and the final result is obtained. This method is faster than evaluating the high-order partial derivatives of the term T/γ. The same holds for the functionals, in which the terms like $1/\sin\theta$ occur or contain the centrifugal potential or acceleration (although the reasons are slightly different here). On the other hand, the price to be paid is the cost of additional memory, since full matrix of $\gamma(r,\theta)$ (or $1/\sin\theta^E$ in the "gradient

approach in ellipsoidal coordinates") has to be stored. The same approach was used for the height anomaly in Balmino et al. (2012), Appendix B.

3. Software presentations

3.1. Description of the software

The aim of this section is to present the new developed software isGrafLab (Irregular Surface GRAvity Field LABoratory), which is modified version of GrafLab 1.1.2 (Bucha and Janák, 2013), and to assess the effectiveness of the gradient approach in spherical and ellipsoidal coordinates. isGrafLab, as well as GrafLab, is written in MATLAB® and equipped with a graphical user interface (GUI), see Fig. 1.

Fig. 1 should be positioned here

The GUI is visually divided into three panels, from which the first and the third panel were changed only slightly. In order to stay brief, for the details about the manipulation with these two panels we would like to advise the reader to Bucha and Janák (2013), Section 3.1.

(i) *Geopotential model and reference system selection*: The only change in this panel is that isGrafLab is not capable to read a variance-covariance matrix of spherical harmonic coefficients as the input file. This option was left out, since the main problem in the computation of commission error is not in the slowness of the computation as much as in the high requirements on the RAM of computer. Thus, the point-wise approach in GrafLab is certainly sufficient.

(ii) *Irregular surface selection*: At first, the *Type of the input coordinates* (ellipsoidal/spherical) must be specified. The grid must be defined by using the seven

self-explanatory arrays in the bottom left of this panel (*Lat.* denotes the latitude and *Lon.* is the longitude). The array *Height above the reference surface (m)* denotes the constant height of the grid above the reference ellipsoid (GRS80 (Moritz, 2000) or WGS84 (NIMA, 2000)) in the case of the ellipsoidal type of the coordinates or above the reference sphere with the radius R, defined by the GGM, in the case of the spherical coordinates. To this surface refer the points $P_0(r_0^E, \theta_0^E, \lambda) \in E$ or $P_0(r_0, \theta, \lambda) \in S$ (see Secs. 2.3 and 2.2, respectively) that will be continued to the irregular surface. By a rule of thumb, to this array one can enter the average value computed from the minimum and the maximum height of the irregular surface above the reference surface (the ellipsoid GRS80/WGS84 or the sphere with the radius R). The entries must be either floating point numbers with decimal points or integer values. Latitudes must be entered within the $\langle -90°, 90° \rangle$ interval and longitudes within the $\langle 0°, 360° \rangle$ or $\langle -180°, 180° \rangle$ interval.

An integer value of the maximum order of the Taylor series ($K \geq 0$) (see Eq. (3)) must be entered into the array *Order of Taylor series:*. If $K = 0$, the functionals are not continued from the regular surface.

Heights of the grid points at the irregular surface must be loaded using the *Browse...* button. In case of the ellipsoidal input coordinates this file must contain the ellipsoidal heights. If the spherical coordinates have been chosen, the spherical radii of the grid points must be given. In both cases, the input file may have two forms:

a) a matrix

$$\begin{bmatrix} (\theta_n, \lambda_1) & \cdots & (\theta_n, \lambda_m) \\ \vdots & \ddots & \vdots \\ (\theta_1, \lambda_1) & \cdots & (\theta_1, \lambda_m) \end{bmatrix},$$

b) a column vector (note the transposition)

$$\left[(\theta_1, \lambda_1) \quad \ldots \quad (\theta_n, \lambda_1) \quad \ldots \quad (\theta_1, \lambda_m) \quad \ldots \quad (\theta_n, \lambda_m)\right]^{\top},$$

where (θ_1, λ_1) are the coordinates of the southernmost and the westernmost grid point (arrays *Lat. min (°)* and *Lon. min (°)*). The northernmost and the easternmost grid point is denoted by (θ_n, λ_m) (arrays *Lat. max (°)* and *Lon. max (°)*). The input file may either be an ASCII file or a binary MAT-file. Points with undefined ellipsoidal heights/spherical radii should be indicated by the value -9999 or NaN. The output values are assigned correspondingly.

(iii) *Calculated parameters and output selection*: From this panel only the check-box *Commission error* was removed. The rest of the panel was left unchanged. For the convenience of the reader, let us herein list again the summary of the functionals that can be computed in isGrafLab, see Table 1. We also note that the formulae to compute each functional can be found in the pdf file Definition_of_functionals_of_the_geopotential_used_in_GrafLab_software.pdf available at [1].

Table 1 should be positioned here

Here, a short note is necessary. The approaches for computing the functionals *Geoid undulation* and *Height anomaly* are the same in isGrafLab as in GrafLab. The reason is that these functionals are referred to particular surfaces, and can not be, by definition, shifted arbitrarily in radial or vertical direction. Moreover, these functionals are computed iteratively as the particular surfaces are not known prior to computation. However, for the convenience of the users we left these

[1] `http://www.svf.stuba.sk/en/departments/department-of-theoretical-geodesy/science-and-research/downloads.html?page_id=4996`

functionals also in isGrafLab.

isGrafLab enables to depict computed data on a map using the Mapping toolbox™ of MATLAB®. For visualizing data using only the basic module of MATLAB®, see e.g. Bezděk and Sebera (2013).

When all the required input parameters and input files have been entered, after clicking the *OK* button, the computation will start. On the left from this button, there is a status line, which provides short explanations during the whole computational process (*Loading GGM file...*, current value of the variable *m* in the order-dependent loop, *Displaying data...*, etc.), so that a user can clearly see in which part of the computation the isGrafLab is. After successful computation, the status *Computation has been finished* will appear. If any of the input parameters or input files have been entered in a wrong format, isGrafLab will open a warning dialog or error dialog with description of the error.

The whole source code of the program called isGrafLab.m is written as a one m-file. A simple flowchart of the program is provided in Fig. 2.

Fig. 2 should be positioned here

3.2. Testing of the gradient approach

The assessment of numerical results obtained from isGrafLab is straightforward. In a test area we computed chosen functionals in isGrafLab with increasing the maximum order of the Taylor series, and compared them to the functionals obtained from GrafLab 1.1.2 using the point-wise approach. These values were assumed to be the reference values at the same points. Differences between the reference values and those obtained from the gradient approach indicate the level of approximation of this method.

Fig. 3 should be positioned here

Let us start with the "gradient approach in ellipsoidal coordinates" at first. For better comparison we will closely follow the test designed by Hirt (2012) with only small modifications. As the test area we used the roughest region on the globe, viz. the part of the Himalayas ($\varphi \in (26°, 29°)$, $\lambda \in (86°, 88°)$, $1'$ spatial resolution) that includes the Mount Everest, see Fig. 3. The topography within this area shows the largest variations on the Earth surface from ~0 km to ~8.8 km. In order to obtain the grid of 180×120 points $P(\varphi, \lambda, h) \in \Sigma$ with ellipsoidal heights of the topography within this area, we used SRTM (Shuttle Radar Topography Mission) digital elevation model Version 4.1 (Jarvis et al., 2008) and the quasi-geoid from EGM2008 (evaluated up to degree 2190 in GrafLab 1.1.2). Note that the SRTM elevations are referred to EGM96 (Lemoine et al., 1998). However, to achieve preferably similar results as in the test by Hirt, we used EGM2008 (see Hirt, 2012, Section 2.4.1). The impact of the choice of the reference surface E to the continued functionals is also described in Hirt (2012). Based on his investigations, herein we used as the regular surface E only the "best" option, i.e. the ellipsoid at the height $h_0 = (\min(h) + \max(h))/2 \approx 4\,\text{km}$ above the reference ellipsoid. At this grid represented by 21 600 points we computed δg_{sa} and T_{rr} for $K = 0, \ldots, 7$ using EGM2008 to degree 2190, and continued them to the Earth surface Σ. Compared to Hirt (2012), in our test we extended the order of the Taylor series from $K = 3$ to $K = 7$ (note that in isGrafLab the value of K can be even larger). The statistical characteristics of this test are shown in Table 2. Fig. 4 gives a graphical representation of the differences for δg_{sa}. The computations were executed on a PC with Intel® Core™ i5-3330 CPU and 4 GB RAM under the 64 bit Windows® 7 OS.

Fig. 4 should be positioned here

Table 2 should be positioned here

Table 2 shows very similar characteristics for δg_{sa} and $K \leq 3$ to those by Hirt (2012), Table 4. It is also obvious that by further increasing the maximum order of the Taylor series beyond $K = 3$, the better approximation of the reference values can be achieved. However, as it was already pointed out in Section 2.3, this convergence has to "stop" at some value of K. This is caused by the approximation of the gradients in the direction of $h - h_0$ by the gradients in the radial direction, see Section 2.3. For $M = 2190$ and the chosen region, the convergence "stops" at $K \approx 5$. However, positive effect of the increased K beyond 3 is evident. For δg_{sa} the RMS fell from 0.23 mGal ($K = 3$) to 0.03 mGal ($K = 5$), and from 0.73 E ($K = 3$) to 0.08 E ($K = 5$) for T_{rr}, which can be considered as significant improvement. These errors are far bellow the commission errors of EGM2008 (Hirt, 2012; Pavlis et al., 2012), therefore this approach can be considered as accurate even in extreme conditions. It should be emphasized that for smaller values of M and/or in smoother areas the results are even more optimistic.

Now let us focus on the "gradient approach in spherical coordinates", in which the convergence never "stops" essentially, since no approximation is used. The ellipsoidal coordinates of the same points $P(\varphi, \lambda, h) \in \Sigma$ within the same area as in the test above were transformed into the spherical coordinates $P(r^E, \theta^E, \lambda) \in \Sigma$. To ensure that the transformed θ^E will be constant along the parallels and subsequently the LCA will be usable, we let $\theta^E = 90^\circ - \varphi$ and obtain the regular grid points $P(r^E, \theta^E, \lambda) \in \Sigma = P(r^E, 90^\circ - \varphi, \lambda) \in \Sigma$. This approximation is admissible, since we are testing only the method herein. Next, we again computed at the points $P(r_0^E, \theta^E, \lambda) \in S$ the functionals δg_{sa}, T_{rr} and their derivatives using

EGM2008 to degree 2190, and continued them from the regular surface S to the surface Σ. The radius r_0^E of the sphere S (see Eq. (3)) was obtained by $r_0^E = (\min(r^E) + \max(r^E))/2 \approx R = 6\,378\,136.3$ m. The order of the Taylor series was set to $K = 0, \ldots, 20$. The results of this test are reported in Table 3.

Table 3 should be positioned here

It is clear that the Taylor series converges now to the reference values, although the convergence "slows down" at $K \approx 15$. In the case that $K = 15$ the RMS is 1.5×10^{-11} mGal for δg_{sa} and 4.7×10^{-11} E for T_{rr}. For smaller values of M the Taylor series converges even faster. Based on these investigations it can be said that for sufficiently high order of the Taylor series the approximation errors of the "gradient approach in spherical coordinates" are negligible.

3.3. Testing of the time efficiency

In this section we assess the time efficiency of the presented software isGrafLab. We compared computation time of the disturbing tensor in the local north-oriented reference frame (LNOF) using isGrafLab and the software presented by Eshagh and Abdollahzadeh (2012). This software is also written in MATLAB® and computes elements of the disturbing tensor at irregular surfaces. In addition, these elements can be evaluated in three different reference frames.

The test was executed on an ordinary PC with Intel® Core™ i5-3330 CPU and 4 GB RAM under the 64 bit Windows® 7 OS. We used EGM2008 to degree 2190 and a global grid at $5' \times 5'$ spatial resolution which corresponds to 9 337 681 points. In isGrafLab we used two sufficiently high orders of the Taylor series (see Table 2), $K = 3$ and $K = 5$. We also applied two of the three available approaches to compute fnALFs in the software (for more details, see Bucha and

Janák, 2013, Section 2.1), namely the standard forward column method (Holmes and Featherstone, 2002) and the extended-range arithmetic (Fukushima, 2012a). The results of the test are summarized in Table 4.

Table 4 should be positioned here

Table 4 reveals that isGrafLab is capable to synthesize the disturbing tensor about 20–10 times faster than the software presented by Eshagh and Abdollahzadeh (2012). On the other hand, their approach computes the disturbing tensor without any approximations, unlike the "gradient approach in *ellipsoidal* coordinates".

4. Summary

The novel developed software isGrafLab (Irregular Surface GRAvity Field LABoratory) has been presented in this paper. isGrafLab is capable to perform fast ultra-high degree SHS at regular spaced grids referring to irregular surfaces, e.g. the Earth surface. The approach implemented in the software was published by Hirt (2012) and also by Balmino et al. (2012). At first, functionals and their derivatives are computed at a regular surface (the sphere or the ellipsoid of revolution) by means of the efficient LCA. Subsequently, the functionals are continued to the irregular surface by applying the Taylor expansion. The order of the Taylor series can be entered by the user. Compared to the "point-wise approach" with two loops that is usually used in this situation, isGrafLab allows accurate and time-saving SHS at dense grids at the Earth surface. The factor of increased computational speed can reach a value of several hundreds. Note that depending on the order of the Taylor series and the number of grid points, in general this

approach involves higher requirements on the RAM of computer compared to the LCA alone. isGrafLab is written in MATLAB® and equipped with an easy-to-use GUI. isGrafLab allows SHS of 38 functionals of the geopotenial employing three different approaches to compute fnALFs with various numerical stability and efficiency (see Bucha and Janák, 2013, Section 2.1).

The numerical investigations have been divided into two separate parts, namely the gradient approach in ellipsoidal and spherical coordinates. It was shown that in the former approach the RMS of the approximation errors can be decreased (compared to Hirt (2012)) by further increasing the maximum order of the Taylor series K. For $K = 5$, the maximum degree $M = 2190$ and the roughest topography on the Earth, viz. the Himalayas, the RMS of the approximation errors reached 0.03 mGal for δg_{sa} and 0.08 E for T_{rr}. As for the later approach, it was demonstrated that sufficiently large order of the Taylor series ensures agreement with the reference values with negligible approximation errors.

Acknowledgements

The work was supported by the national projects VEGA 1/1092/11 and APVV-0072-11. The first author would like to gratefully thank Aleš Bezděk and Josef Sebera for the fruitful and valuable discussions on GrafLab and isGrafLab. The authors are grateful to Christian Hirt for recommending this topic to us. Thanks are extended to the anonymous referees for their valuable comments on the manuscript and the software.

References

Adams, J.C., Swarztrauber, P.N., 1997. SPHEREPACK 2.0: A Model Development Facility. NCAR Technical Note NCAR/TN-436-STR, 58 pp.

Balmino, G., Vales, N., Bonvalot, S., Briais, A., 2012. Spherical harmonic modelling to ultra-high degree of Bouguer and isostatic anomalies. Journal of Geodesy 86, 499–520. doi: 10.1007/s00190-011-0533-4.

Barthelmes, F., 2003. Calculation Service under ICGEM (International Centre for Global Earth Models). `http://icgem.gfz-potsdam.de/ICGEM/`, (accessed 7 February, 2013).

Barthelmes, F., 2013. Definition of functionals of the geopotential and their calculation from spherical harmonic models: Theory and formulas used by the calculation service of the International Centre for Global Earth Models (ICGEM), `http://icgem.gfz-potsdam.de`. Scientific Technical Report STR09/02. GFZ German Research Centre for Geosciences. Potsdam, Germany, 32 pp.

Bezděk, A., Sebera, J., 2013. Matlab script for 3D visualizing geodata on a rotating globe. Computers and Geosciences 56, 127–130. doi: 10.1016/j.cageo.2013.03.007.

Bucha, B., Janák, J., 2013. A MATLAB-based graphical user interface program for computing functionals of the geopotential up to ultra-high degrees and orders. Computers and Geosciences 56, 186–196. doi: 10.1016/j.cageo.2013.03.012.

Cheong, H.B., Park, J.R., Kang, H.G., 2012. Fourier-series representation and

425 projection of spherical harmonic functions. Journal of Geodesy 86, 975–990.
426 doi: 10.1007/s00190-012-0558-3.

427 Colombo, O.L., 1981. Numerical methods for harmonic analysis on the sphere.
428 Report No. 310. Department of Geodetic Science and Surveying, The Ohio
429 State University. Columbus, Ohio, 140 pp.

430 Eshagh, M., Abdollahzadeh, M., 2012. Software for generating gravity gradients
431 using a geopotential model based on an irregular semivectorization algorithm.
432 Computers and Geosciences 39, 152–160. doi: 10.1016/j.cageo.2011.06.003.

433 Fantino, E., Casotto, S., 2009. Methods of harmonic synthesis for global geopo-
434 tential models and their first-, second- and third-order gradients. Journal of
435 Geodesy 83, 595–619. doi: 10.1007/s00190-008-0275-0.

436 Finlay, C.C., Maus, S., Beggan, C.D., Bondar, T.N., Chambodut, A., Cher-
437 nova, T.A., Chulliat, A., Golovkov, V.P., Hamilton, B., Hamoudi, M., Holme,
438 R., Hulot, G., Kuang, W., Langlais, B., Lesur, V., Lowes, F.J., Lühr, H.,
439 Macmillan, S., Mandea, M., McLean, S., Manoj, C., Menvielle, M., Michaelis,
440 I., Olsen, N., Rauberg, J., Rother, M., Sabaka, T.J., Tangborn, A., Tøffner-
441 Clausen, L., Thébault, E., Thomson, A.W.P., Wardinski, I., Wei, Z., Zvereva,
442 T.I., 2010. International geomagnetic reference field: The eleventh genera-
443 tion. Geophysical Journal International 183, 1216–1230. doi: 10.1111/j.1365-
444 246X.2010.04804.x.

445 Förste, C., Bruinsma, S., Shako, R., Marty, J.C., Flechtner, F., Abrikosov, O.,
446 Dahle, C., Lemoine, J.M., Neumayer, H., Biancale, R., Barthelmes, F., König,
447 R., Balmino, G., 2011. EIGEN-6 A new combined global gravity field model

including GOCE data from the collaboration of GFZ-Potsdam and GRGS-Toulouse, in: EGU General Assembly, Vienna, Austria, 3-8 April.

Förste, C., Bruinsma, S.L., Flechtner, F., Marty, J.C., Lemoine, J.M., Dahle, C., Abrikosov, O., Neumayer, H., Biancale, R., Barthelmes, F., Balmino, G., 2012. A new release of EIGEN-6C, in: AGU Fall Meeting, San Francisco, USA, 3-7 December.

Freeden, W., Schreiner, M., 2009. Spherical Functions of Mathematical Geosciences: A Scalar, Vectorial, and Tensorial Setup. Springer-Verlag, Berlin Heidelberg, 602 pp.

Fukushima, T., 2012a. Numerical computation of spherical harmonics of arbitrary degree and order by extending exponent of floating point numbers. Journal of Geodesy 86, 271–285. doi: 10.1007/s00190-011-0519-2.

Fukushima, T., 2012b. Numerical computation of spherical harmonics of arbitrary degree and order by extending exponent of floating point numbers: II first-, second-, and third-order derivatives. Journal of Geodesy 86, 1019–1028. doi: 10.1007/s00190-012-0561-8.

Gruber, C., Novák, P., Sebera, J., 2011. FFT-based high-performance spherical harmonic transformation. Studia Geophysica et Geodaetica 55, 489–500. doi: 10.1007/s11200-011-0029-y.

Hirt, C., 2012. Efficient and accurate high-degree spherical harmonic synthesis of gravity field functionals at the Earth's surface using the gradient approach. Journal of Geodesy 86, 729–744. doi: 10.1007/s00190-012-0550-y.

Hobson, E.W., 1931. The Theory of Spherical and Ellipsoidal Harmonics. Cambridge University Press, Cambridge, Great Britain, 500 pp.

Hoffmann-Wellenhof, B., Moritz, H., 2005. Physical Geodesy. Springer, Wien, New York, 403 pp.

Holmes, S.A., Featherstone, W.E., 2002. A unified approach to the Clenshaw summation and the recursive computation of very high degree and order normalised associated Legendre functions. Journal of Geodesy 76, 279–299. doi: 10.1007/s00190-002-0216-2.

Holmes, S.A., Pavlis, N.K., 2008. Spherical harmonic synthesis software Harmonic_synth. `http://earth-info.nga.mil/GandG/wgs84/gravitymod/new_egm/new_egm.html`, (accessed 5 December, 2012).

Janák, J., Šprlák, M., 2006. New software for gravity field modelling using spherical harmonics. Geodetic and Cartographic Horizon 52, 1–8 (in Slovak).

Jarvis, A., Reuter, H.I., Nelson, A., Guevara, E., 2008. Hole-filled SRTM for the globe Version 4. Available from the CGIAR-CSI SRTM 90m Database (`http://srtm.csi.cgiar.org`).

Jekeli, C., Lee, J.K., Kwon, J.H., 2007. On the computation and approximation of ultra-high-degree spherical harmonic series. Journal of Geodesy 81, 603–615. doi: 10.1007/s00190-006-0123-z.

Lemoine, F.G., Kenyon, S.C., Factor, J.K., Trimmer, R.G., Pavlis, N.K., Chinn, D.S., Cox, C.M., Klosko, S.M., Luthcke, S.B., Torrence, M.H., Wang, Y.M., Williamson, R.G., Pavlis, E.C., Rapp, R.H., Olson, T.R., 1998.

The Development of the Joint NASA GSFC and the National Imagery and Mapping Agency (NIMA) Geopotential Model EGM96. Technical Report NASA/TP1998206861. National Aeronautics and Space Administration. USA, 582 pp.

Moritz, H., 2000. Geodetic reference system 1980. Journal of Geodesy 74, 128–162. doi: 10.1007/s001900050278.

National Imagery and Mapping Agency (NIMA), 2000. World Geodetic System 1984: Its Definition and Relationships with Local Geodetic Systems. Technical Report No. NIMA TR8350.2. National Imagery and Mapping Agency. USA, 175 pp.

Nesvadba, O., 2009. Numerical problems in evaluating high degree and order associated Legendre functions, in: General Assembly of the European Geosciences Union, Vienna, Austria, 19-24 April.

Pavlis, N.K., Holmes, S.A., Kenyon, S.C., Factor, J.K., 2012. The development and evaluation of the Earth Gravitational Model 2008 (EGM2008). Journal of Geophysical Research 117(B04406), 1–38. doi: 10.1029/2011JB008916.

Rapp, R.H., 1997. Use of potential coefficient models for geoid undulation determinations using a spherical harmonic representation of the height anomaly/geoid undulation difference. Journal of Geodesy 71, 282–289.

Sanso, F., Sona, G., 2001. ELGRAM: an Ellipsoidal Gravity Model Manipulator. Bollettino di Geodesia e Scienze Affini 60, 3, 215–226.

Smith, D.A., 1998. There is no such thing as “the” EGM96 geoid: subtle points on the use of a global geopotetial model. IGeS Bulletin 8, 17–28.

Smith, J.M., Olver, F.W.J., Lozier, D.W., 1981. Extended-range arithmetic and normalized Legendre polynomials. ACM Trans Math Softw 7, 93–105.

Sneeuw, N., 1994. Global spherical harmonic analysis by least-squares and numerical quadrature methods in historical perspective. Geophysical Journal International 118, 707–716.

Tscherning, C.C., Rapp, R.H., Goad, C., 1983. A comparison of methods for computing gravimetric quantities from high degree spherical harmonic expansions. Manuscripta Geodaetica 8, 249–272.

Šprlák, M., 2011. On the numerical problems of spherical harmonics: numerical and algebraic methods avoiding instabilities of associated Legendre's functions. ZFV - Zeitschrift für Geodäsie, Geoinformation und Landmanagement 136, 310–320.

Wenzel, G., 1998. Ultra-high degree geopotential models GPM98A, B and C to degree 1800, in: Joint meeting of the International Gravity Commission and International Geoid Commission, Trieste, Italy, 7-12 September.

Wieczorek, M., 2012. SHTOOLS – Tools for working with spherical harmonics. `http://shtools.ipgp.fr/`, (accessed 28 November, 2013).

Wittwer, T., Klees, R., Seitz, K., Heck, B., 2008. Ultra-high degree spherical harmonic analysis and synthesis using extended-range arithmetic. Journal of Geodesy 82, 223–229. doi: 10.1007/s00190-007-0172-y.

List of Tables

List of Figures

Table 1: Functionals of the geopotential available in isGrafLab. Explanation of the symbols in the table: V – gravitational potential, W – gravity potential, g – gravity, T – disturbing potential, δg – gravity disturbance, Δg – gravity anomaly, ξ – north-south component of deflection of the vertical, η – east-west component of deflection of the vertical, Θ – total deflection of the vertical, N – geoid undulation, ζ_{Ell} – generalized height anomaly, ζ – height anomaly; the subscript *sa* denotes the spherical approximation of the functional; (r, θ, λ) stands for the spherical coordinates; (x, y, z) denotes the coordinates in the local north-oriented reference frame; the subscripts $r, \theta, \lambda, x, y, z$ and their combinations stand for the derivatives of the functionals with respect to the particular coordinate; the number in the superscript denotes computational demand (computation time of the functional and memory usage during the computation) – (1) small, (2) medium, (3) high, (4) very high; $^{(*)}$ and $^{(**)}$ denote the functionals for which the value of $n_{\min}$ cannot be larger than 2 and 0, respectively.

Actual field	Disturbing field	Geometrical characteristics of the actual field
$V^{(1)}$	$T^{(1)}$	$\xi^{(2)}$
$V^{(3)}_{rr}, V^{(3)}_{\theta\theta}, V^{(3)}_{\lambda\lambda}$	$T^{(3)}_{rr}, T^{(3)}_{\theta\theta}, T^{(3)}_{\lambda\lambda}$	$\eta^{(1)}$
$V^{(3)}_{r\theta}, V^{(3)}_{r\lambda}, V^{(3)}_{\theta\lambda}$	$T^{(3)}_{r\theta}, T^{(3)}_{r\lambda}, T^{(3)}_{\theta\lambda}$	$\Theta^{(2)}$
$V^{(3)}_{xx}, V^{(3)}_{yy}, V^{(3)}_{zz}$	$T^{(3)}_{xx}, T^{(3)}_{yy}, T^{(3)}_{zz}$	$^{(*)}N^{(2)}$
$^{(*)}V^{(4)}_{xy}, {}^{(*)}V^{(4)}_{xz}, {}^{(*)}V^{(4)}_{yz}$	$^{(*)}T^{(4)}_{xy}, {}^{(*)}T^{(4)}_{xz}, {}^{(*)}T^{(4)}_{yz}$	$\zeta^{(1)}_{Ell}$
$W^{(1)}$	$^{(**)}\delta g^{(3)}$	$^{(*)}\zeta^{(2)}$
$g^{(2)}$	$\delta g^{(1)}_{sa}$	
$g^{(1)}_{sa}$	$\Delta g^{(1)}_{sa}$	
$W^{(1)}_{rr}$	$T^{(1)}_{rr}$	

Table 2: Statistical characteristics of differences between the reference values and those obtained using the "gradient approach in ellipsoidal coordinates"; used EGM2008 to degree 2190; gravity disturbances are in mGal (1 mGal = 10^{-5} m s^{-2}), second radial derivatives of disturbing potential in 1 E = 10^{-9} s^{-2} and CPU time in s.

	δg_{sa}					T_{rr}				
	Min	Max	Mean	RMS	CPU time	Min	Max	Mean	RMS	CPU time
Reference − (0th order)	−101.661	46.375	−6.712	14.6743	11	−183.224	103.589	−5.797	27.0377	11
Reference − (0th + 1st order)	−23.622	38.123	−0.285	3.3007	13	−61.617	95.468	−0.431	8.9100	14
Reference − (0th to 2nd order)	−14.390	3.973	−0.131	0.8870	16	−41.712	14.055	−0.290	2.7115	17
Reference − (0th to 3rd order)	−1.749	4.564	−0.016	0.2293	18	−5.255	13.911	−0.029	0.7280	18
Reference − (0th to 4th order)	−1.200	0.319	−0.008	0.0609	20	−3.744	1.125	−0.009	0.1832	21
Reference − (0th to 5th order)	−0.213	0.264	−0.005	0.0320	23	−0.449	0.830	0.000	0.0766	24
Reference − (0th to 6th order)	−0.195	0.132	−0.004	0.0297	26	−0.401	0.354	0.000	0.0672	26
Reference − (0th to 7th order)	−0.192	0.131	−0.004	0.0296	29	−0.396	0.350	0.000	0.0666	28

Table 3: Statistical characteristics of differences between the reference values and those obtained using the "gradient approach in spherical coordinates"; used EGM2008 to degree 2190; gravity disturbances are in mGal, second radial derivatives of disturbing potential in E and CPU time in s.

	δg_{sa}					T_{rr}				
	Min	Max	Mean	RMS	CPU time	Min	Max	Mean	RMS	CPU time
Reference – (0th order)	−101.0	102.9	−3.8	17.2	15	−284.3	241.1	−1.8	35.7	14
Reference – (0th to 2nd order)	−11.0	9.6	-2.4×10^{-2}	1.4	19	−30.1	26.8	-2.1×10^{-2}	4.3	18
Reference – (0th to 5th order)	−0.1	0.1	7.8×10^{-5}	1.8×10^{-2}	27	−0.4	0.4	-1.8×10^{-4}	6.0×10^{-2}	25
Reference – (0th to 10th order)	-1.3×10^{-5}	9.8×10^{-6}	3.8×10^{-9}	1.4×10^{-6}	38	-4.2×10^{-5}	3.2×10^{-5}	1.0×10^{-10}	4.6×10^{-6}	38
Reference – (0th to 15th order)	-1.5×10^{-10}	1.2×10^{-10}	2.4×10^{-14}	1.5×10^{-11}	49	-4.7×10^{-10}	3.6×10^{-10}	1.2×10^{-13}	4.7×10^{-11}	46
Reference – (0th to 20th order)	-4.8×10^{-11}	4.3×10^{-11}	-1.8×10^{-14}	4.8×10^{-12}	60	-9.8×10^{-11}	1.2×10^{-10}	-1.3×10^{-14}	9.4×10^{-12}	56

Table 4: Computation time of the full disturbing tensor in the LNOF at 9 337 681 points using isGrafLab and the software presented by Eshagh and Abdollahzadeh (2012); used EGM2008 to degree 2190; K – the maximum order of the Taylor series; SFCM, ERA – the standard forward column method, the extended-range arithmetic, respectively (two of the three approaches for computing fnALFs in isGrafLab).

	isGrafLab ($K = 3$) SFCM / ERA	isGrafLab ($K = 5$) SFCM / ERA	Eshagh and Abdollahzadeh
CPU time (h)	0.7 / 1.0	1.1 / 1.5	13.4

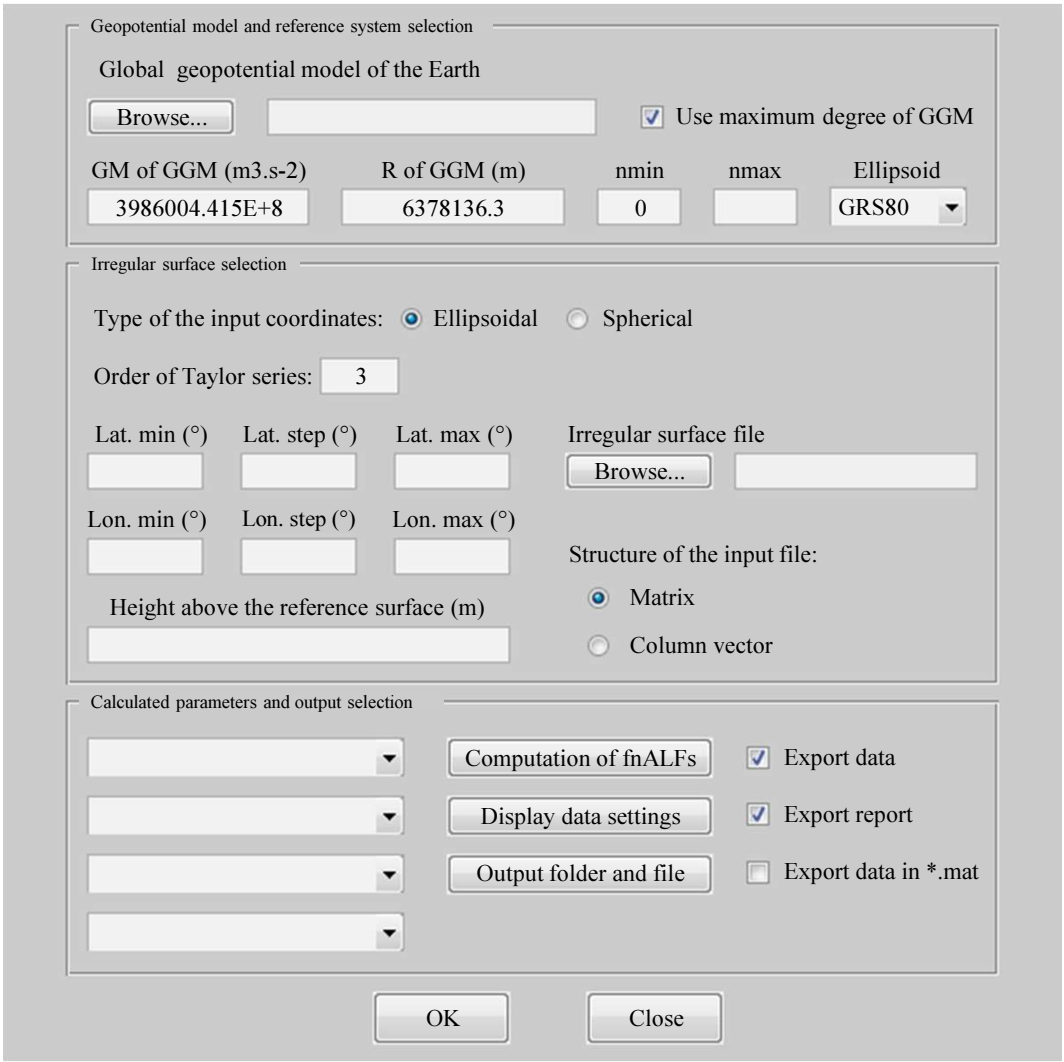

Figure 1: isGrafLab graphical user interface.

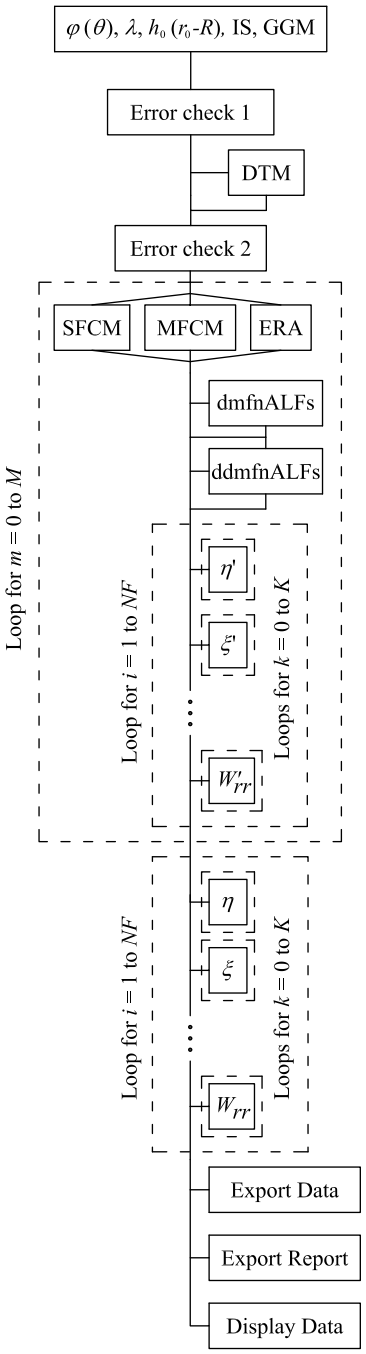

Figure 2: Flowchart of the isGrafLab. Explanation of the symbols and abbreviations in the flowchart: φ $(\theta), \lambda$ – ellipsoidal (spherical) coordinates of the evaluation points, h_0 $(r_0 - R)$ – height of the regular surface above the reference ellipsoid (sphere), IS – input file containing the heights of the irregular surface, GGM – global geopotential model of the Earth; Error check 1 – the first error check of the input data; DTM – digital terrain model; Error check 2 – the second error check of the input data; SFCM, MFCM, ERA – computation of the modified fnALFs using the standard forward column method, the modified forward column method or the extended-range arithmetic approach, respectively; dmfnALFs – computation of the first-order derivatives of

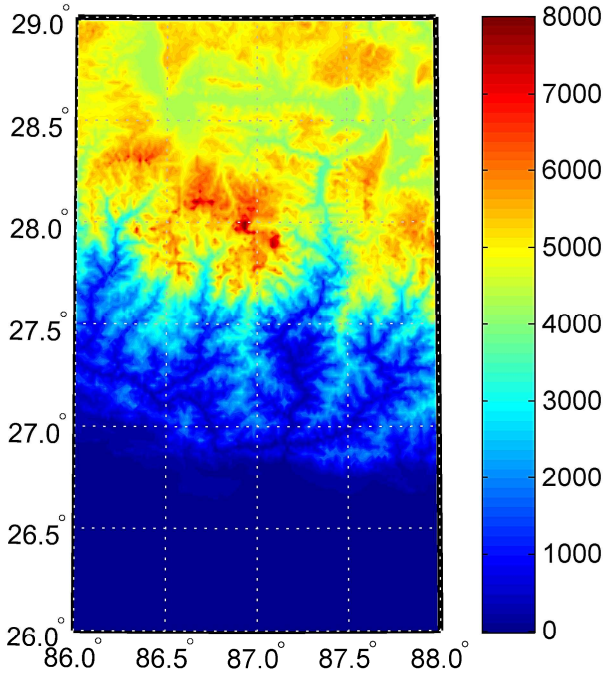

Figure 3: Topography of the Himalayas within the region $\varphi \in (26°, 29°)$, $\lambda \in (86°, 88°)$ at $1'$ spatial resolution. Units in metres.

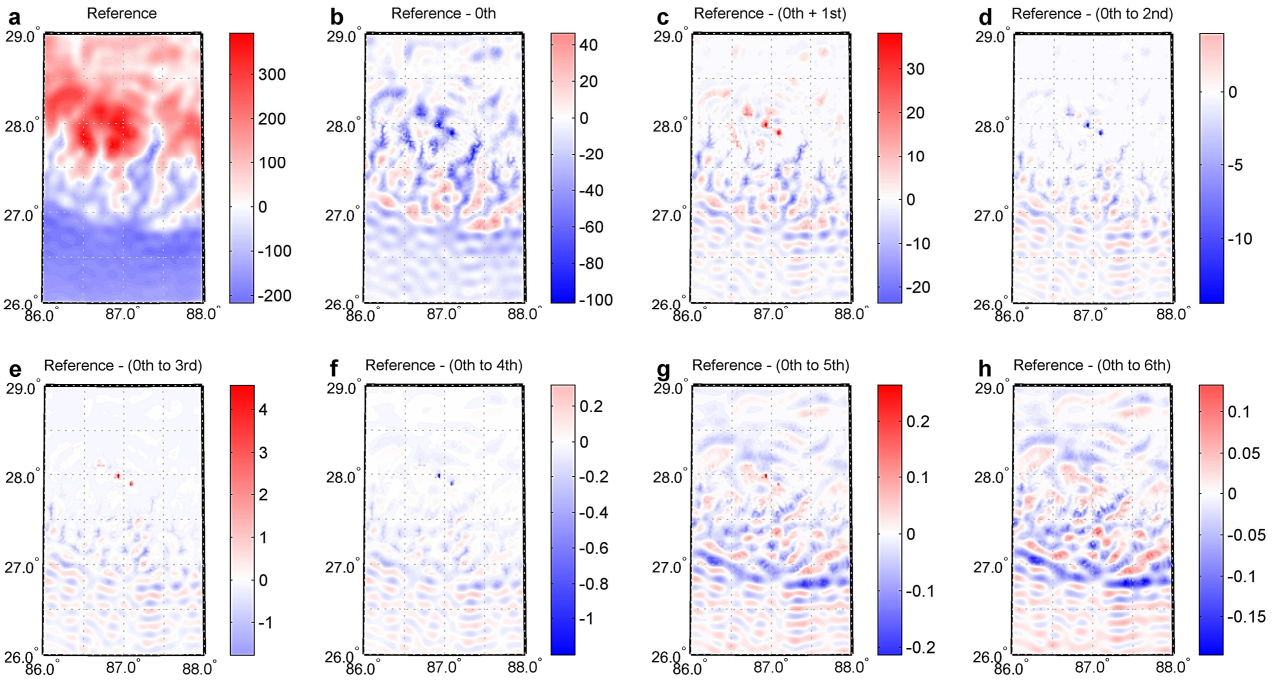

Figure 4: **a** Reference gravity disturbances in spherical approximation over the Himalayas, **b** – **h** differences between the reference and the approximated gravity disturbances in spherical approximation using the orders of the Taylor series $K = 0, \ldots, 6$. Units in mGal.